

# Estimating Tibial Stress throughout the Duration of a Treadmill Run

HANNAH RICE<sup>1,2</sup>, GILLIAN WEIR<sup>2</sup>, MATTHIEU B. TRUDEAU<sup>3</sup>, STACEY MEARDON<sup>4</sup>,  
TIMOTHY DERRICK<sup>5</sup>, and JOSEPH HAMILL<sup>2</sup>

<sup>1</sup>*Sport and Health Sciences, University of Exeter, Exeter, UNITED KINGDOM;* <sup>2</sup>*Biomechanics Laboratory, University of Massachusetts, Amherst, MA;* <sup>3</sup>*Human Performance Laboratory, Brooks Running Company, Seattle, WA;* <sup>4</sup>*Department of Physical Therapy, East Carolina University, NC;* and <sup>5</sup>*Department of Kinesiology, Iowa State University, IA*

## ABSTRACT

RICE, H., G. WEIR, M. B. TRUDEAU, S. MEARDON, T. DERRICK, and J. HAMILL. Estimating Tibial Stress throughout the Duration of a Treadmill Run. *Med. Sci. Sports Exerc.*, Vol. 51, No. 11, pp. 2257–2264, 2019. **Introduction:** Stress fractures of the tibia are a problematic injury among runners of all levels. Quantifying tibial stress using a modeling approach provides an alternative to invasive assessments that may be used to detect changes in tibial stress during running. This study aimed to assess the repeatability of a tibial stress model and to use this model to quantify changes in tibial stress that occur throughout the course of a 40-min prolonged treadmill run. **Methods:** Synchronized force and kinematic data were collected during prolonged treadmill running from 14 recreational male rearfoot runners on two separate occasions. During each session, participants ran at their preferred speed for two consecutive 20-min runs, separated by a 2-min pause. The tibia was modeled as a hollow ellipse and bending moments and stresses at the distal third of the tibia were estimated using beam theory combined with inverse dynamics and musculoskeletal modeling. **Results:** Intraclass correlation coefficients indicated good-to-excellent repeatability for peak stress values between sessions. Peak anterior and posterior stresses increased after 20 min of prolonged treadmill running and were 15% and 12% greater, respectively, after 40 min of running compared with the start of the run. **Conclusion:** The hollow elliptical tibial model presented is a repeatable tool that can be utilized to assess within-participant changes in peak tibial stress during running. The increased stresses observed during a prolonged treadmill run may have implications for the development of tibial stress fracture. **Key Words:** TIBIAL STRESS, OVERUSE INJURY, RUNNING, MUSCULOSKELETAL MODELING, BEAM THEORY

Running is an accessible and increasingly popular form of physical activity that is associated with reduced mortality (1–4). However, there is a high incidence of injury among runners (5,6) with two thirds of recreational runners reportedly sustaining an injury over a 2-yr period (6). Bone stress injuries are one of the more problematic injuries due in part to their lengthy recovery time and the most severe of these—stress fractures—have been reported to comprise up to 30% of running-related injuries (7). The tibia is one of the most common sites of lower limb stress fracture among runners (8–10).

The magnitudes of tibial stress during physical activities such as running and jumping are typically far below the failure threshold (11–13) but may result in the accumulation of microdamage. Microdamage is a natural consequence

of loading in healthy bone. However, in an attempt to remove microdamage, bone undergoes “targeted remodeling” and this results in temporarily increased porosity (14). This can impair the mechanical properties of bone (15), increasing susceptibility to a stress fracture. Stress fractures are thought to occur due to the accumulation of microdamage without adequate repair (16).

The total stress on a loaded bone results from a combination of axial and bending forces acting on the bone. Both external loads and muscular forces act on the bone and contribute to axial and bending forces. Pauwels’ Theorem suggests that the external loads tend to bend the bone in one direction while the forces applied by the muscles tend to bend the bone in the opposite direction (17). The resultant bending places one surface of the bone under tension and the opposite surface under compression. However, the stress due to the bending is superimposed with the stress due to longitudinal compression. This increases the compression on the compressed surface even further while reducing the tension on the tensile surface.

Existing studies have provided contradictory information regarding the net direction of bending during the support phase of the human running gait cycle (18–23). Most recent studies (18,22,23), including one that directly measured bone deformation using surgically implanted bone screws (21), have indicated that the resultant bending moment (due to the combined effect of the internal muscular forces and external

Address for correspondence: Hannah Rice, Ph.D., Sport and Health Sciences, Richards Building, St Luke’s Campus, Heavitree Rd, Exeter, EX1 2LU, United Kingdom. E-mail: H.Rice@exeter.ac.uk

Submitted for publication February 2019.

Accepted for publication May 2019.

0195-9131/19/5111-2257/0

MEDICINE & SCIENCE IN SPORTS & EXERCISE®

Copyright © 2019 by the American College of Sports Medicine

DOI: 10.1249/MSS.0000000000002039

reaction forces) about the medial–lateral axis tends to bend the tibia in a concave posterior manner during running stance, thus placing the posterior tibia under compression. Experimental data, including *in vivo* bone strain estimates, have shown increased bone strain after prolonged physical activity (24–26), indicative of an association between fatigue and bone strain. It is unknown to what extent tibial stress magnitudes change throughout the duration of a prolonged run and this is likely important in understanding the risk of stress fractures in runners in an ecological setting.

The use of invasive estimates of human bone strain is justifiably limited. Biomechanical models provide a valuable non-invasive alternative that allow specific research questions to be addressed. Existing tibial modeling approaches have used beam theory to estimate tibial bending (19,20) and stress (18,22,23), where a cross-section of the tibia was modeled as a hollow ellipse. Peak tibial stress estimates obtained using beam theory were highly correlated with more computationally expensive finite element model estimates during walking ( $r > 0.9$ ), but were found to underestimate the values (23). This suggests that beam theory estimates are a useful tool to assess within-subject changes in peak stress. However the repeatability of this approach has not been quantified.

Therefore, the aims of this study were to quantify the repeatability of beam theory estimates of tibial stress during running and to assess to what extent tibial stress changes throughout the duration of a prolonged treadmill run. It was hypothesized that the stresses acting at the anterior and posterior peripheries of the tibia would be relatively more repeatable than those at the medial and lateral peripheries. It was also hypothesized that the magnitude of stress would increase throughout the 40-min treadmill run.

## METHODS

### Participants

Fourteen recreationally active male participants were included in the study (mean (standard deviation (SD)): 24.4 (4.4) yr; 70.2 (7.6) kg; 1.78 (0.05) m). Participants were habitual rearfoot striking recreational runners who ran a minimum of 15 miles per week. All participants were injury-free at the time of data collection and had no history of serious lower limb injury within the previous year. All participants provided written informed consent before participation in this study which was approved by the University of Massachusetts Amherst Institutional Review Board.

### Experimental Setup

Retro-reflective markers were positioned to identify pelvis, thigh, lower leg and foot segments as detailed by Weir et al. (27). All markers were positioned by the same investigator. Markers were secured using double-sided tape followed by Fixomull tape (Smith & Nephew, London, UK) and an athletic stretch tape (Jaybird and Mais, Lawrence, MA) intended to minimize marker movement. Height and body mass were

recorded for scaling of the model. Synchronized kinematic (8-camera motion capture system, Oqus 5; Qualysis, Inc., Gothenburg, Sweden; 200 Hz) and ground reaction force data from a force instrumented treadmill (Treadmetrix, Park City, UT; 2000 Hz) were obtained during running.

### Protocol

Participants completed two prolonged treadmill running data collection sessions in the Biomechanics Laboratory exactly 1 wk apart at the same time of day on each occasion. This study was part of a larger study examining the influence of footwear on running gait (27). In the present study, participants ran in a neutral shoe (Brooks Defyance 9, Seattle, WA) that was new to them. Participants first undertook a warm-up run for 5 min during which their preferred running speed for a 40-min training run was determined. The treadmill was initially set at the participants' self-reported speed and increased/decreased until the participant settled on a comfortable speed. The same running speed was utilized in the second session. After the warm-up, a standing calibration trial was obtained while participants stood on the treadmill.

The prolonged treadmill run involved two 20-min runs at the preferred speed (group mean: 3.4 [0.3] m·s<sup>-1</sup>) that were separated by a 2-min period during which participants changed into a second shoe of identical construction but of a different color and a second standing trial was collected. Retroreflective markers had been positioned on the second shoe during the initial setup. Participants ran for 1 min to become accustomed to the running speed and footwear before the 20-min period commenced in each of the running sessions. Data were collected for 30 s at the start (minute 0) and end (minute 20) of the first bout, and at the end (minute 40) of the second bout of running. Data were also collected at the start of the second bout of running to provide information regarding potential recovery effects of the 2-min pause. This time point was not included in the main analyses.

### Data Analysis

Kinematic and force data were filtered with a zero-lag fourth-order low pass Butterworth filter at 8 Hz. Three-dimensional kinematic and kinetic data were processed using Visual3D software (C-motion, Inc., Rockville, MD). Ten stance phases per participant were analyzed from each time point. Data were time normalized to 101 points. A customized Matlab (R2017a; Mathworks, Natick, MA) program was written to estimate tibial stress. The tibia was modeled as a hollow elliptical beam (18,22,23) using elliptical geometry with diameters obtained from Franklyn et al. (28) (outer medial–lateral, 23.22 mm; outer anterior–posterior, 29.32 mm; inner medial–lateral, 10.08 mm; inner anterior–posterior, 9.76 mm). Segment center of mass accelerations and joint reaction forces were calculated. The contribution to bending from nine muscles that span the cross-section of interest (distal third of tibia) were included in the model (tibialis anterior, soleus, tibialis posterior, extensor digitorum longus, flexor digitorum longus, flexor

hallucis longus, peroneus brevis, peroneus longus, extensor hallucis longus). The contributions of the two gastrocnemii muscles that span the tibial cross-section but originate on the femur were considered through inclusion of the knee joint moment. Muscle definitions were obtained from the Hamner model (29). The muscle line of action was used to determine the angle between the muscular force and the tibia. Where the muscle included only origin and insertion coordinates, the straight line between these coordinates was used. Where wrapping points existed, the longest line between two adjacent coordinates was used. Dynamic muscle forces were estimated using static optimization with a cost function minimizing the sum of cubed muscle stresses—a cost function widely used for lower extremity analysis (30). Nonlinear cost functions allow more load sharing across muscles than linear cost functions (31). Sagittal plane hip, knee and ankle moments were constrained to be equal to those obtained through inverse dynamics. Maximum isometric muscular forces were determined using physiological cross-sectional areas (PCSA) from Arnold et al. (32) and maximum dynamic muscular forces were constrained by the product of the PCSA, a specific tension of  $61 \text{ N} \cdot \text{cm}^{-2}$  (32) and an eccentric plateau of 1.5 (33). Moment arms for each muscle were determined as a function of sagittal plane ankle angle during stance from the Hamner model (29). The axial and bending contributions from each muscle were calculated in both the anterior–posterior and medial–lateral directions.

Normal stresses at the posterior, anterior, lateral, and medial peripheries were calculated as axial stress plus/minus bending stress. These stress values were determined using the following:

1. For each point of stance, axial and bending forces due to the external reaction forces and internal muscular forces were vector summed to represent the resultant axial force acting at or about the centroid at the distal third of the tibia.
2. Axial stresses were estimated by dividing the resultant axial force by the cross-sectional area of the hollow ellipse.
3. For each point of stance, the resultant bending moment was the sum of the bending due to the internal muscular forces and the external reaction forces acting on the centroid at the distal third of the tibia. The bending due to the muscles crossing the centroid was determined by multiplying the muscular forces by the respective moment arms. The bending at the centroid due to the external reaction forces included the contributions from both the knee joint reaction force and the knee joint moment.
4. Anterior–posterior bending stresses were estimated by multiplying the resultant bending moment about the medial–lateral axis of the cross-section by the distance to the ellipse anterior/posterior periphery and dividing by the area moment of inertia of the hollow ellipse about its medial–lateral axis.
5. Medial–lateral bending stresses were estimated by multiplying the resultant bending moment about the anterior–posterior axis of the cross-section by the distance to the ellipse medial/lateral periphery and dividing by the area moment of inertia of the hollow ellipse about its anterior–posterior axis.

## Statistical Analysis

**Model repeatability.** Repeatability was assessed using data from minute 0 of the two runs conducted a week apart. One participant was excluded from the repeatability analysis due to a technical issue during their second visit. Average and percentage differences in peak stress between sessions were obtained and coefficient of variation (CV) was determined to indicate variability of peak stress in relation to the mean value. The intraclass correlation coefficient (ICC) was used to assess test-retest reliability with a two-way mixed-effects, single-measurement model with absolute agreement (34). A value of 0.75 to 0.90 was indicative of good repeatability and a value greater than 0.90 was indicative of excellent repeatability (34). Bland–Altman 95% limits of agreement gave the range within which 95% of differences between repeat peak stress values were expected to lie (35).

**Assessment of tibial bending moments and tibial stress throughout the run.** The influence of run duration on tibial bending moments and tibial stress was assessed using data from the 40-min running session in which participants wore the neutral shoe (see Weir et al. (27) for further explanation relating to the session that was not included in the present study). This was assessed using a repeated measures ANOVA with three time points: minute 0, minute 20, and minute 40. Mauchly's test was used to assess sphericity and the Greenhouse–Geisser correction was applied where the assumption of sphericity was violated. *Post hoc* paired *t*-tests were conducted in the case of a main effect to identify whether differences existed between minute 0 and minute 20, and minute 0 and minute 40 with a Bonferroni correction ( $\alpha = 0.05/2$ ). Where there was a main effect, differences between the end of bout 1 (minute 20) and the start of bout 2 were also assessed using paired *t*-tests to provide an indication as to whether the pause in running to change footwear influenced the findings. The statistical analyses outlined above were used both to assess normalized time histories and to assess peak values, with the former utilizing statistical parametric mapping (SPM). The SPM analyses were carried out using open-source spm1d Matlab code (<http://www.spm1d.org> (36)).

## RESULTS

**Model repeatability.** Peak bending moments and stress values are presented in Table 1. The ICC values indicated excellent repeatability for peak bending moments and good-to-excellent repeatability for peak stress values. Smaller percentage differences and CV values were observed between sessions for peak stress in the anterior and posterior directions than the medial and lateral directions. The Bland–Altman limits of agreement showed that an increase in anterior stress of less than 18.3 MPa and in posterior stress (increase in negative direction) of less than 19.0 MPa would be expected in 95% of repeat measurements.

**Bending moments.** Resultant bending moments about the medial–lateral axis (contributing to anterior–posterior stress) were predominantly in the positive anticlockwise

TABLE 1. Sessions 1 and 2 mean, standard deviation, and repeatability outcomes for peak bending moments and peak stresses at the distal third of the tibia during running.

	Mean	SD	Between-Session Difference		CV	ICC	Bland–Altman Limits of Agreement
Resultant bending moments (N·m)							
ML axis	106.2	26.5	4.0	3.8%	0.2	0.806	−28.0, 36.0
	110.2	25.5					
AP axis	43.6	17.0	0.8	1.9%	0.4	0.887	−11.9, 22.2
	42.8	15.4					
Stresses (MPa)							
Anterior	43.8	12.3	2.0	5.1%	0.3	0.765	−13.8, 18.3
	46.1	11.6					
Posterior	−66.5	15.2	−2.2	3.0%	0.2	0.836	−19.0, 15.0
	−68.5	14.8					
Medial	12.4	8.9	3.5	29.3%	0.7	0.839	−10.6, 5.0
	9.6	7.4					
Lateral	−23.6	12.7	−2.8	17.5%	0.5	0.717	−13.0, 20.1
	−20.1	10.4					

AP, anterior-posterior; ML, medial-lateral.

direction throughout stance (Figure 1A), interpreted as tending to bend the tibia in a concave posterior manner (Figure 1B). Peak bending stress contributed 82.3% (2.3%) to peak posterior compressive stress. Resultant bending moments about the anterior-posterior axis were predominantly in the positive clockwise direction throughout stance (Figure 1C),

interpreted as tending to bend the tibia in a concave medial manner (Figure 1D).

**Assessment of tibial bending moments and tibial stress throughout the run.** The SPM analyses revealed a main effect for run duration on resultant bending about the medial-lateral axis (36%–38% stance,  $P = 0.020$ ; 43%–48%

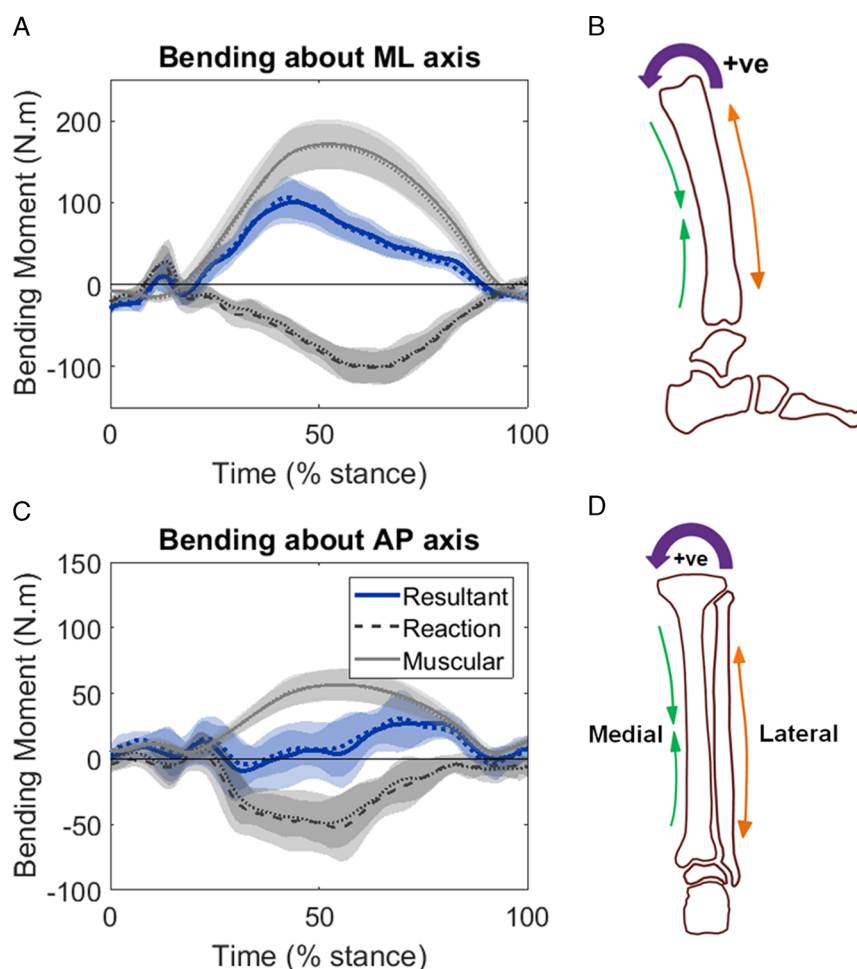


**FIGURE 1**—Mean and standard deviation time histories of bending moments about the medial-lateral axis (A) and anterior-posterior axis (C) during stance in two separate data collection sessions (minute 0). Positive bending moment indicates posterior (B) and medial (D) compression. Shading around the mean curve represents the standard deviation. *Solid lines* and *dashed lines* represent the first and second repeat data collection sessions, respectively.



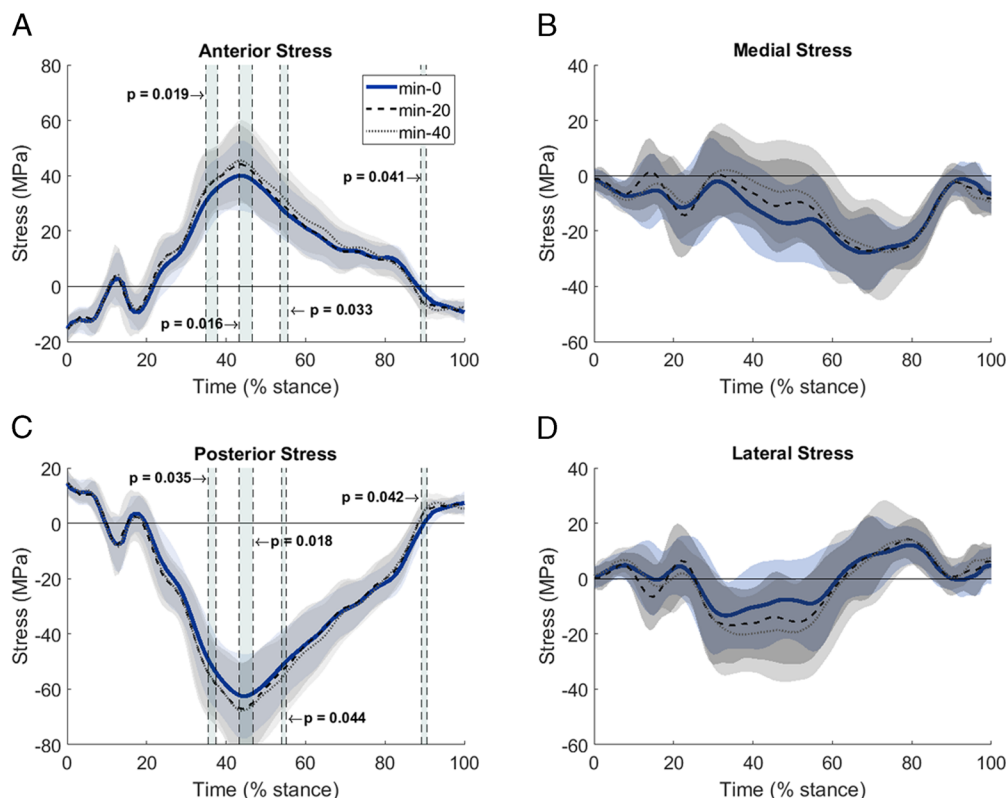


**FIGURE 2**—Stresses at the anterior (A), posterior (C), medial (B) and lateral (D) peripheries during stance. *Vertical shaded areas indicate the time points during stance in which there was a main effect for run duration (A, C). Shading around the mean curve represents the standard deviation.*

stance,  $P = 0.002$ ; 52%–56% stance,  $P = 0.006$ ). *Post hoc* SPM paired  $t$ -tests showed resultant bending moments were increased from minute 0 to minute 40 of the run (36%–37% of stance:  $P = 0.012$ ). There were no differences from minute 0 to minute 20. There were no differences between minute 20 and the start of bout 2. There was no main effect for duration on resultant bending about the anterior–posterior axis. SPM analyses revealed a main effect for duration on both anterior and posterior stresses (Figure 2). *Post hoc* SPM paired  $t$ -tests showed that anterior stresses increased from minute 0 to minute 40 (36%–37% of stance:  $P = 0.005$ ). Posterior stresses increased from minute 0 to minute 20 (46% of stance:  $P = 0.02$ ). There were no differences in anterior or posterior stresses between minute 20 and the start of bout 2. There was no main effect for duration on medial or lateral stresses.

**Assessment of peak tibial bending moments and peak tibial stress.** Peak bending moments at the three time points throughout the run are presented in Table 2. Sphericity was assumed for bending moments about both axes. There was a main effect for duration on peak resultant bending about the medial–lateral axis ( $F_{(2)} = 15.314$ ,  $P < 0.001$ ). *Post hoc* paired samples  $t$ -tests revealed significantly greater peak resultant bending moments during minute 20 ( $P = 0.001$ ) and minute 40 ( $P < 0.001$ ) than minute 0. There was no difference in peak resultant bending moment between minute 20 and the start of bout 2 ( $P = 0.253$ ). There was no main effect for duration on peak resultant bending moments about the anterior–posterior axis ( $F_{(2)} = 0.770$ ,  $P = 0.473$ ).

Peak stress values at the three time points throughout the run are presented in Table 2. Sphericity was assumed for anterior, posterior and medial stresses, but was violated for lateral stress so the Greenhouse–Geisser adjustment was used. There was a main effect for duration on peak anterior stress ( $F_{(2)} = 15.592$ ,  $P < 0.001$ ) and posterior stress ( $F_{(2)} = 14.976$ ,  $P < 0.001$ ). *Post hoc* paired samples  $t$ -tests revealed that peak anterior stress was greater during minute 20, and minute 40 than minute 0 (both  $P < 0.001$ ) and peak posterior stress was greater at minute 20 ( $P = 0.001$ ) and minute 40 ( $P < 0.001$ ) than minute 0. There were no differences in peak anterior stress or posterior stress between minute 20 and the start of bout 2 ( $P = 0.292$  and  $P = 0.238$ , respectively). There was no main effect for duration on peak medial ( $F_{(2)} = 1.656$ ,  $P = 0.210$ ) or lateral stress ( $F_{(2)} = 3.336$ ,  $P = 0.076$ ). Individual percentage changes in peak anterior and posterior stress from minute 0 are presented in Figure 3. Thirteen of the 14 participants showed increased peak anterior stress over time,

**TABLE 2.** Mean (SD) peak tibial bending moments and tibial stress values.

	Minute 0	Minute 20	Minute 40
Resultant bending moments (N-m)			
ML axis	104.0 (26.8)	113.4 (31.5)*	116.3 (32.9)*
AP axis	43.1 (16.4)	46.1 (18.6)	43.0 (22.4)
Stresses (MPa)			
Anterior	42.8 (12.4)	47.4 (14.8)*	49.1 (15.5)*
Posterior	-65.2 (15.4)	-70.4 (17.9)*	-72.7 (18.6)*
Medial	11.9 (8.7)	15.6 (8.8)	15.7 (9.7)
Lateral	-22.6 (12.7)	-28.3 (12.9)	-29.8 (15.7)

\*Significantly different from minute 0.

and 12 of the 14 showed increased peak posterior stress over time.

## DISCUSSION

This study estimated tibial stress during running using beam theory, assessing both the repeatability of the measurement and changes in stress that occur throughout a 40-min treadmill run. The resultant bending moment about the medial–lateral axis tended to bend the tibia in a concave posterior manner, indicative of predominantly tensile stresses on the anterior tibia and compressive stresses on the posterior tibia during stance. This supports previous studies using a similar model (18,22,23) and the bone deformation that was observed when assessed using bone screws during running (21). The resultant bending moment about the anterior–posterior axis tended to bend the tibia in a concave medial manner, indicative of predominantly tensile stresses on the lateral tibia and compressive stresses on the medial tibia during stance. This is also consistent with the bone deformation observed during running (21) indicating that the model used in the present study is a useful representation of bone bending. The magnitudes of stress at the anterior and posterior peripheries compare well with those reported during running by Meardon et al. (22). Additionally, the greatest peak stresses occurred posteriorly, in agreement with Meardon et al. (18,22). The majority of stress fractures are reported to occur in the posterior medial tibia (37–39), thus estimating bone stress using beam theory appears to have convergent validity.

The repeatability assessment provides reference data for peak bending moments and peak stress values during running

when collected in two separate sessions. In support of the hypotheses, peak stresses at the anterior and posterior peripheries were relatively more repeatable between sessions than at the medial and lateral peripheries. Thus, within-participant changes in peak stress at the anterior or posterior tibia are likely more detectable than at the medial or lateral tibia. The high ICC values provide confidence in the repeatability of this modeling approach. The Bland–Altman 95% limits of agreement provide an estimate of the difference from the mean value within which 95% of day-to-day repeats would be expected to lie and are not suitable to determine clinical relevance.

In support of the second hypothesis, there were increases in peak anterior and posterior stress from minute 20 of the run onwards in comparison to minute 0. Participants from the present study perceived the run to be of moderate intensity (RPE, 10–12 [27]). **This increased stress over the course of the prolonged run supports previous findings of increased bone strain after physical activity (24–26)** despite the protocol of the present study being less physically demanding. The average within-session increases in peak anterior and posterior stress were 15% and 12%, respectively, by the end of the run (~6–7 MPa). These differences were three times greater than the mean between-session (repeatability) differences. Increased peak anterior and posterior stresses were observed in 12 of the 14 participants, providing confidence that the overall increases observed were not due to chance. **Meardon et al. (18) found that runners with a history of tibial stress fracture had anterior and posterior peak stress values that were 11.4 MPa (19%) and 12.0 MPa (13%) greater, respectively, than those with no history of the injury.** These differences were sufficient

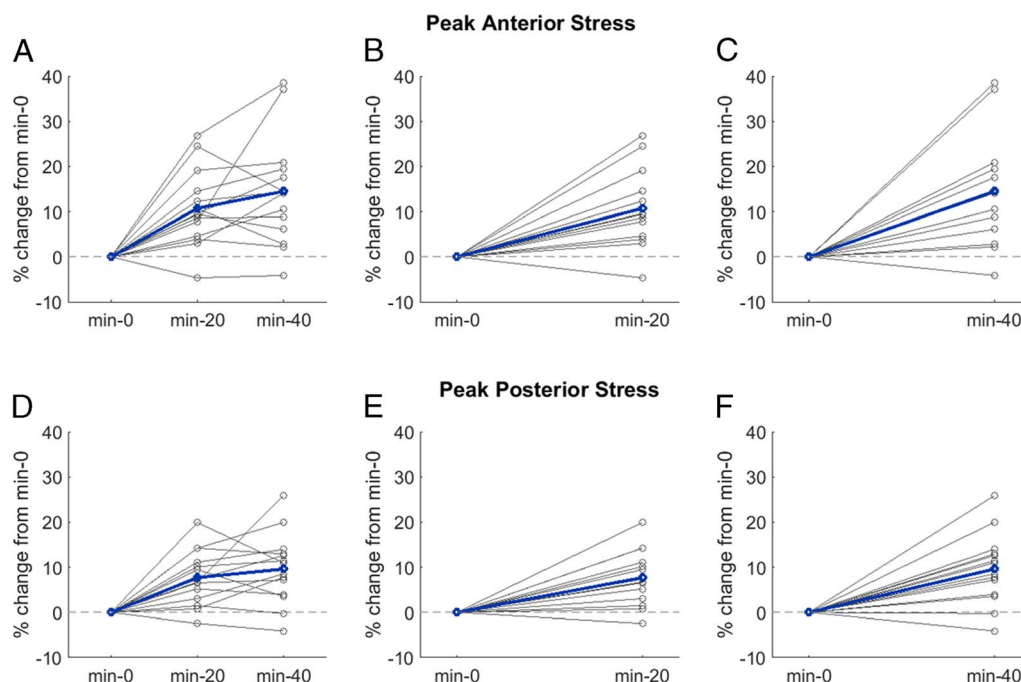


**FIGURE 3—Peak anterior (A, B, C) and posterior (D, E, F) stresses over time. Line graphs display percentage change in individual peak stress values throughout the entire run (A, D). Changes in peak stress from minute 0 to minute 20 (B, E) and from minute 0 to minute 40 (C, F) are presented separately for clarity. Bold, blue lines represent group mean changes over time.**

to distinguish between two clinically meaningful groups and should therefore be considered to be clinically relevant. This previous study involved a different population and used data collection procedures that differed from the present study. Additionally, the control group in the previous study displayed greater standard deviations in anterior and posterior peak stress values than in the present study. Thus, the magnitude of change observed in the present study within a single moderate run is likely to be clinically relevant.

The present study showed that increased peak anterior–posterior tibial stresses during the first 20 min of a moderate treadmill run were approximately maintained for the remaining 20 min. It is not clear how quickly after the start of the run these changes occurred or whether they would have plateaued or further increased had the run been of a longer duration. Furthermore, a run of greater intensity may have induced greater increases in peak tibial stress. An understanding of these factors can inform the design of running-based training programs in the future. A possible mechanistic explanation for the increased stresses observed is a reduced ability of the planar flexor muscles to counter the external dorsiflexor moment through eccentric contraction as a result of muscular fatigue.

The threshold of “excessive” tibial stress is unknown. However, the repetitive nature of running and the relatively high occurrence of tibial stress injuries among distance runners would suggest that the increases in peak anterior–posterior tibial stress of 12% to 15% per step observed in the present study could have a considerable cumulative effect that may increase the risk of overuse injury. Identification of interventions that minimize or delay the onset of these stress increases is warranted.

**Limitations.** Modeling the tibia as a hollow elliptical beam provides a worthwhile tool for identifying within-participant changes in stress. The model itself necessarily has numerous limitations and the absolute magnitudes of stress reported should be considered with this in mind. The elliptical model was scaled to each participant’s height and mass but is combined with existing model data that are not participant-specific.

Estimating muscular forces through static optimization provides an indicator of the relative contributions from each muscle but is subject to assumptions related to the maximal force capability and neural control strategies. In terms of the data collection protocol, the pause at the half way point of the run may have introduced alterations to running gait. The fact that no difference in bending moments or stress values existed between minute 20 and the start of bout 2 of the run provides reassurance that this did not influence the overall findings.

The participants in the present study were all male, habitual rearfoot striking runners. Runners with a more anterior foot strike pattern may not demonstrate the same increases in stress during a treadmill run as observed here, and similarly it cannot be assumed that the same findings would be observed in females. Although runners in the present study had no notable lower-limb injuries within the previous year, a more thorough interrogation of previous injury history would provide further assurances that the results are not influenced by this factor.

## CONCLUSIONS

Estimating peak tibial stress during running using beam theory modeling was found to be a repeatable approach that provides a useful tool to quantify within-participant changes in tibial stress. In the present study, increased anterior tension and posterior compression of the tibia occurred within the first half of a moderate treadmill run, and these increases were maintained throughout the second half of the run. The increased stresses observed during a prolonged treadmill run may have implications for the development of tibial stress fracture.

The authors would like to thank Dr Carl Jewell and Dr Hannah Wyatt for their invaluable contributions to this work.

This research was supported by Brooks Running Company, Seattle, WA, USA. The authors declare no conflicts of interest. The results of the study are presented clearly, honestly, and without fabrication, falsification, or inappropriate data manipulation. The results of the present study do not constitute endorsement by ACSM.

## REFERENCES

1. Chakravarty EF, Hubert HB, Lingala VB, Fries JF. Reduced disability and mortality among aging runners: a 21-year longitudinal study. *Arch Intern Med.* 2008;168(15):1638–46.
2. Lee D-C, Pate RR, Lavie CJ, Sui X, Church TS, Blair SN. Leisure-time running reduces all-cause and cardiovascular mortality risk. *J Am Coll Cardiol.* 2014;64(5):472–81.
3. Schnohr P, Marott JL, Lange P, Jensen GB. Longevity in male and female joggers: the Copenhagen City Heart Study. *Am J Epidemiol.* 2013;177(7):683–9.
4. Wang N, Zhang X, Xiang Y-B, et al. Associations of Tai Chi, walking, and jogging with mortality in Chinese men. *Am J Epidemiol.* 2013;178(5):791–6.
5. van Gent RN, Siem D, van Middelkoop M, van Os AG, Bierma-Zeinstra SM, Koes BW. Incidence and determinants of lower extremity running injuries in long distance runners: a systematic review. *Br J Sports Med.* 2007;41(8):469–80.
6. Messier SP, Martin DF, Mihalko SL, et al. A 2-year prospective cohort study of overuse running injuries: The Runners and Injury Longitudinal Study (TRAILS). *Am J Sports Med.* 2018;46(9):2211–21.
7. Robertson GA, Wood AM. Lower limb stress fractures in sport: optimising their management and outcome. *World J Orthop.* 2017; 8(3):242–55.
8. Iwamoto J, Takeda T. Stress fractures in athletes: review of 196 cases. *J Orthop Sci.* 2003;8(3):273–8.
9. Brukner P, Bradshaw C, Khan KM, White S, Crossley K. Stress fractures: a review of 180 cases. *Clin J Sport Med.* 1996;6(2): 85–9.
10. Kiel J, Kaiser K. Stress Reaction and Fractures. *StatPearls*. Treasure Island (FL): StatPearls Publishing; 2018.
11. Burr DB, Milgrom C, Fyhrie D, et al. In vivo measurement of human tibial strains during vigorous activity. *Bone.* 1996;18(5): 405–10.
12. Milgrom C, Finestone A, Simkin A, et al. In-vivo strain measurements to evaluate the strengthening potential of exercises on the tibial bone. *J Bone Joint Surg Br.* 2000;82(4):591–4.
13. Milgrom C, Finestone A, Levi Y, et al. Do high impact exercises produce higher tibial strains than running? *Br J Sports Med.* 2000;34(3): 195–9.

14. Hughes JM, Popp KL, Yanovich R, Bouxsein ML, Matheny RW. The role of adaptive bone formation in the etiology of stress fracture. *Exp Biol Med (Maywood)*. 2017;242(9):897–906.
15. Burr DB, Turner CH, Naick P, et al. Does microdamage accumulation affect the mechanical properties of bone? *J Biomech*. 1998;31(4):337–45.
16. Burr DB. Why bones bend but don't break. *J Musculoskelet Neural Interact*. 2011;11(4):270–85.
17. Pauwels F. *Biomechanics of the Locomotor Apparatus: Contributions on the Functional Anatomy of the Locomotor Apparatus*. Berlin Heidelberg: Springer-Verlag; 1980.
18. Meardon SA, Willson JD, Gries SR, Kemozek TW, Derrick TR. Bone stress in runners with tibial stress fracture. *Clin Biomech (Bristol, Avon)*. 2015;30(9):895–902.
19. Haris Phuah A, Schache AG, Crossley KM, Wrigley TV, Creaby MW. Sagittal plane bending moments acting on the lower leg during running. *Gait Posture*. 2010;31(2):218–22.
20. Scott SH, Winter DA. Internal forces of chronic running injury sites. *Med Sci Sports Exerc*. 1990;22(3):357–69.
21. Yang P-F, Sanno M, Ganse B, et al. Torsion and antero-posterior bending in the in vivo human tibia loading regimes during walking and running. *PLoS One*. 2014;9(4):e94525.
22. Meardon SA, Derrick TR. Effect of step width manipulation on tibial stress during running. *J Biomech*. 2014;47(11):2738–44.
23. Derrick TR, Edwards WB, Fellin RE, Seay JF. An integrative modeling approach for the efficient estimation of cross sectional tibial stresses during locomotion. *J Biomech*. 2016;49(3):429–35.
24. Yoshikawa T, Mori S, Santiesteban AJ, et al. The effects of muscle fatigue on bone strain. *J Exp Biol*. 1994;188(1):217–33.
25. Milgrom C, Radeva-Petrova D, Finestone A, et al. The effect of muscle fatigue on in vivo tibial strains. *J Biomech*. 2007;40(4):845–50.
26. Arndt A, Ekenman I, Westblad P, Lundberg A. Effects of fatigue and load variation on metatarsal deformation measured in vivo during barefoot walking. *J Biomech*. 2002;35(5):621–8.
27. Weir G, Jewell C, Wyatt H, et al. The influence of prolonged running and footwear on lower extremity biomechanics. *Footwear Sci*. 2019;11(1):1–11.
28. Franklyn M, Oakes B, Field B, Wells P, Morgan D. Section modulus is the optimum geometric predictor for stress fractures and medial tibial stress syndrome in both male and female athletes. *Am J Sports Med*. 2008;36(6):1179–89.
29. Hamner SR, Seth A, Delp SL. Muscle contributions to propulsion and support during running. *J Biomech*. 2010;43(14):2709–16.
30. Erdemir A, McLean S, Herzog W, van den Bogert AJ. Model-based estimation of muscle forces exerted during movements. *Clinical Biomechanics*. 2007;22(2):131–54.
31. Pedersen DR, Brand RA, Cheng C, Arora JS. Direct comparison of muscle force predictions using linear and nonlinear programming. *J Biomech Eng*. 1987;109(3):192–9.
32. Arnold EM, Ward SR, Lieber RL, Delp SL. A model of the lower limb for analysis of human movement. *Ann Biomed Eng*. 2010;38(2):269–79.
33. Hasson CJ, Miller RH, Caldwell GE. Contractile and elastic ankle joint muscular properties in young and older adults. *PLoS One*. 2011;6(1):e15953.
34. Koo TK, Li MY. A guideline of selecting and reporting intraclass correlation coefficients for reliability research. *J Chiropr Med*. 2016;15(2):155–63.
35. Bland JM, Altman DG. Measuring agreement in method comparison studies. *Stat Methods Med Res*. 1999;8(2):135–60.
36. Pataky TC, Robinson MA, Vanrenterghem J. Region-of-interest analyses of one-dimensional biomechanical trajectories: bridging 0D and 1D theory, augmenting statistical power. *PeerJ*. 2016;4:e2652.
37. Devas MB. Stress fractures of the tibia in athletes or shin soreness. *J Bone Joint Surg Br*. 1958;40-B(2):227–39.
38. Fredericson M, Bergman AG, Hoffman KL, Dillingham MS. Tibial stress reaction in runners: correlation of clinical symptoms and scintigraphy with a new magnetic resonance imaging grading system. *Am J Sports Med*. 1995;23(4):472–81.
39. Nattiv A, Kennedy G, Barrack MT, et al. Correlation of MRI grading of bone stress injuries with clinical risk factors and return to play: a 5-year prospective study in collegiate track and field athletes. *Am J Sports Med*. 2013;41(8):1930–41.